Biochemical and Biophysical Research Communications **286,** 1204–1211 (2001)
doi:10.1006/bbrc.2001.5526, available online at http://www.idealibrary.com on IDEAL®

# 3D Model for TM Region of the AT-1 Receptor in Complex with Angiotensin II Independently Validated by Site-Directed Mutagenesis Data

Gregory V. Nikiforovich[1] and Garland R. Marshall
*Department of Biochemistry and Molecular Biophysics, Campus Box 8036, Washington University, St. Louis, Missouri 63110,*

Received June 29, 2001

**A three-dimensional model of the complex of angiotensin II (AII) with the transmembrane (TM) region of the angiotensin II receptor of type 1 (the AT-1 receptor) was obtained by molecular modeling procedures employing structural homology to the X-ray structure of rhodopsin. Since the modeling procedure considered only steric and energy considerations without prior knowledge of the experimental results of site-directed mutagenesis, the results with receptor mutants could be used for independent validation of the model. Indeed, the model brings in contact the residues of AII responsible for agonistic activity, Tyr[4], His[6], and Phe[8], with many residues of AT-1 involved in signal transduction according to site-directed mutagenesis. The model also predicts the existence of several possible conformational pathways for transferring the binding signal through the TM region of AT-1 to the intracellular loops interacting with the G-protein.** © 2001 Academic Press

*Key Words:* **angiotensin II; angiotensin receptors; G-protein coupled receptors; molecular modeling.**

The octapeptide angiotensin II (Asp[1]-Arg[2]-Val[3]-Tyr[4]-Ile/Val[5]-His[6]-Pro[7]-Phe[8], AII) interacts mainly with two specific receptor proteins, AT-1 and AT-2 (1). Out of these two, AT-1 is the primary vascular receptor associated with blood pressure regulation. It mediates virtually all of the known physiological actions of AII in cardiovascular, renal, neuronal, endocrine, hepatic, and other target cells (1). AT-1 receptors are highly homologous between various species (up to 95% (2)). AT-1 also has high homology with rhodopsin (Rh) and with the other members of the rhodopsin family of the G-protein-coupled receptors (GPCRs); see, e.g., (3). Therefore, the study of molecular mechanisms involved in AII–AT-1 interaction benefits rational design of new ligands of AT-1 and new mutants of that receptor, and also serves as a valuable prototype for the entire rhodopsin family of GPCRs.

Molecular determinants of the AII–AT-1 interaction are present both in the peptide ligand as well as the transmembrane receptor. On the ligand side, many very extensive structure–activity studies with AII analogs (e.g., (4, 5) and references therein) showed that the moieties indispensable both for binding to the AT-1 receptor and for initiating signal transduction are the side chains of Tyr[4], His[6], Phe[8], and the C-terminal carboxyl. Phe[8] is especially important for agonistic activity: a single replacement of Phe[8] for an aliphatic residue, as Ile[8], results in an AII antagonist (4). The three-dimensional (3D) structure of the octapeptide AII has been repeatedly studied by many physicochemical methods including NMR, CD, IR, etc. (though not X-ray crystallography; the only exception was the complex of AII with an antibody (6)). Several 3D models of the "receptor-bound" conformation of AII have been suggested by molecular modeling and NMR spectroscopy of rigidified analogs of AII. We have developed one of these models previously (7, 8); this model became widely accepted in AII and AT-1 studies by other authors (3, 9, 10).

On the receptor side, during the last several years, a variety of mutants of AT-1 have been expressed and tested for ligand binding and for inositol phosphate (IP) production (for reviews see, e.g., (9, 11)). More than 40 residues in AT-1 have been shown to be sensitive either to ligand binding or to signal transduction (see Table 1). In structural terms, AT-1 belongs to the so-called 7-transmembrane (7TM) proteins whose transmembrane part consists mainly of the 7-helical bundle. Very few experimental data are available on the 3D structure of AT-1. They include studies on the isolated AT-1 fragments (e.g., (12)), and some recent experimental studies employing the AII analogs with

[1] To whom correspondence should be addressed. Fax: 1-314-362-0234. E-mail: gregory@ccb.wustl.edu.

0006-291X/01 $35.00

**TABLE 1**

Summary of Biological Testing Results for AT-1 Mutants

```
         10        20        30        40        50        60
          |         |         |         |         |         |
MALNSSAEDGIKRIQDDCPKAGRHSYIFVMIPTLYSIIFVVGIFGNSLVVIVIYFYMKLK
         70        80        90       100       110       120
          |         |         |         |         |         |
TVASVFLLNLALADLCFLLTLPLWAVYTAMEYRWPFGNHLCKIASASVSFNLYASVFLLT
        130       140       150       160       170       180
          |         |         |         |         |         |
CLSIDRYLAIVHPMKSRLRRTMLVAKVTCIIIWLMAGLASLPAVIHRNVYFIENTNITVC
        190       200       210       220       230       240
          |         |         |         |         |         |
AFHYESRNSTLPIGLGLTKNILGFLFPFLIILTSYTLIWKALKKAYEIQKNKPRNDDIFR
        250       260       270       280       290       300
          |         |         |         |         |         |
IIMAIVLFFFFSWVPHQIFTFLDVLIQLGVIHDCKISDIVDTAMPITICIAYFNNCLNPL
        310       320       330       340       350     359
          |         |         |         |         |       |
FYGFLGKKFKKYFLQLLKYIPPKAKSHSSLSTKMSTLSYRPSDNMSSSAKKPASCFEVE
```

*Note.* TM helical regions are underlined. Residues known to be involved in extracellular ligand binding are shown in bold italics, in intracellular ligand binding in plain letters, in signal transduction in bold plain letters.

individual amino acid substitutions for Bpa (*p*-benzoyl-L-phenylalanyne, a photoreactive label) (13–15). The latter studies indicate that Bpa[1] on AII may bind the AT-1 receptor at the 166–199 region, Bpa[8] at the 285–295 region (14), and Bpa[3] may contact position 172 (13).

The data of site-directed mutagenesis have been used as basis for several 3D models of the AT-1 receptor and its complexes with the ligands developed by molecular modeling. The early models have been constructed based on 3D structure of bacteriorhodopsin (BR); it is commonly accepted now that BR is not a good "template" for GPCRs, since it has low-to-no homology to this family (16) and the relative orientation of transmembrane segments is different. The more recent models are based on the 3D structure of Rh that was revealed by electronic microscopy (17) or, in much more detail, by recent X-ray crystallography (18). In all cases, however, the models have been built by placing an appropriate 3D structure of a ligand (mainly AII) in direct contact with residues of AT-1 occupying positions known to be most sensitive either to ligand binding, or to signal transduction. In this way, the data of site-directed mutagenesis for the AT-1 receptor could not be used for independent validation of the models in question, since this information was already incorporated in the models. Therefore, this study presents a 3D model of the complex between AII and the TM region of AT-1 built by molecular modeling employing only considerations of energy calculations and steric complementarity. Though not including the loop regions at this stage, such a model allows independent validation by comparison with the available data of site-directed mutagenesis.

## METHODS

*TM helical bundle of AT-1.* Transmembrane helical fragments have been located in the sequence of the rat AT-1 receptor by sequence homology to the Rh helices found by the CLUSTAL W procedure (the URL address http://ca.expasy.org/tools). The endpoints of helices were refined by the nonstatistical procedure developed by us earlier (19). The helical fragments have been assembled in a TM helical bundle following the procedure of "enhanced homology modeling," which consists of (i) determining conformations of individual helices by independent energy minimization involving all dihedral angles; (ii) superimposing the obtained conformations over the X-ray structure of Rh (18) according to sequence homology and, (iii) packing helices by finding the energetically best arrangement of the individual helices, in which dihedral angles of the backbone are "frozen" in the values obtained earlier. Accordingly, the variables for the packing procedure are the dihedral angles of the side chains for all helices, which are optimized by the algorithm developed earlier (20) as well as the $6 \times 7 = 42$ additional "global" parameters corresponding to movements of each helix as a rigid body. The packing procedure is described in detail elsewhere (21). The "global" starting point for assembling the TM bundle for AT-1 has been that of the X-ray structure of Rh (18). Energy calculations used the ECEPP force field (22, 23); the electrostatic term was omitted to avoid artifacts in helix packing due to its interfacial location and the complexity of the local dielectric.

*Complex of AII and the TM region of AT-1.* The "receptor-bound" conformation of AII deduced by us earlier (structure II from Table 2 in (7)) has been docked to the developed 3D model of TM helical bundle of AT-1 by the GRAMM molecular-docking procedure available at the URL address http://reco3.musc.edu. The suggested 3D model of AII specifies the "receptor-bound" conformation of the $Val^3$-$Tyr^4$-Ile/$Val^5$-$His^6$-$Pro^7$-$Phe^8$-COOH fragment of AII; we have assumed that the N-terminal fragment of AII, $NH_2$-$Asp^1$-$Arg^2$, adopts an energetically favorable extended conformation. First, 1000 low-scoring configurations of AII within the TM helical bundle of AT-1 have been found using a low-resolution "gray" option of the GRAMM procedure (the option developed in our lab earlier (24); the employed GRAMM parameters were as follows: mmode = generic; eta = 3.8; ro = 6.5; fr = 0.0; crang = grid_step; ccti = grey; crep = all; maxm =

**TABLE 2**

Residues of AT-1 in Contact with Residues of AII

| | AT-1 residues | | | |
|---|---|---|---|---|
| AII residues | Family 1 | Family 2 | Family 3 | Family 4 |
| Asp[1] | **L112,** F204, F248, F249, S252, A291, **N294** | M284 | **S115, L118,** L119, **I245,** F249, ***N295,*** N298 | **H256, *T260,*** T287, I288, A291 |
| Arg[2] | V108, **N111, L112, S115,** F204, A291, **N294, *N295,*** N298 | Y87, S105 | **L112, S115, I245,** F248, F249, S252, **N294, *N295,*** N298 | **N111, L112, S115,** I288, A291, ***N295*** |
| Val[3] | S252, **H256,** Q257, ***T260,*** T287, A291 | L197, N200, F261 | **L112,** V116, G203, F204, F249, S252, **W253** | W84, ***T260,*** I288 |
| **Tyr[4]** | V108, S109, **L112, *T260,*** F261 | S105, S109, **L112,** N200, Q257 | **L112,** N200, S252, Q257, A291 | W84, V108, S109, **L112,** F204 |
| Val[5] | ***T260,*** F261 | **L112,** N200, G203, F204, S252, Q257 | N200, I201, F204, Q257 | Y87, S105 |
| **His[6]** | — | **L112,** V116, F249, S252, **W253** | L197, Q257, F261 | S105 |
| Pro[7] | G196, L197, N200, F261 | V108, **H256, *T260,*** A291 | V108, S109, **L112,** N200, I288 | L197, N200 |
| **Phe[8]** | A163, **I193,** G196 | **N111,** F248, S252, **H256,** A291, **Y292, N294, *N295*** | W84, S105, S109, M284, I288 | Y113, **I193,** G196, L197, N200 |
| **COOH** | **P162,** A163 | **F77, N111, Y292, *N295*** | W84, M284, I288 | Y113, A163, G196, N200 |

*Note.* Residues of AT-1 known to be involved in signal transduction or constitutive activity are shown in bold, those involved in ligand binding are shown in bold italics.

1000, and ai = 20). These configurations were considered further as possible starting points for energy minimization of the entire complex. The configurations without a significant number of possible sterical clashes were selected as the actual starting points for energy minimization performed by the same computational procedure used previously for helix packing. In this case, however, the procedure involved independent movements in the space of $6 \times 8 = 48$ "global" parameters (seven helices plus AII) as well as optimization of the dihedral angles of the side chains for all helices and AII by the algorithm developed earlier (20).

## RESULTS AND DISCUSSION

### *3D Models for the Complex of AII and TM region of AT-1*

Our procedure for helix packing has been validated earlier by packing TM helices of BR (21). Starting from the "global" parameters corresponding to the X-ray structure of BR (25), energy minimization reproduced a TM bundle that differed from the X-ray structure by the rmsd value of only 1.14 Å (the rmsd values calculated for C$\alpha$ atoms are mentioned here and further throughout the text). For AT-1, helical fragments have been identified as described above (see the underlined segments in Table 1). They have been packed in a bundle that differed from the initial X-ray structure of Rh by the rmsd value of 2.5 Å.

The GRAMM procedure obtained 1000 low-scoring configurations for the complex of AII and AT-1. The 100 configurations with the most favorable values of the GRAMM scoring function all concentrated in the spatial position at the extracellular "entry" into the TM helical bundle differing mainly by their general orientation of the N-terminal end of AII "outside" or "inside" the bundle. Out of top 50, only 19 configurations possessed less than 10 close contacts (<3 Å) between the backbone atoms of AT-1 and AII. Those 19 configurations have been selected as the starting points for energy minimization. Since our energy estimations were performed for a large complex (about 160 residues altogether), and did not account for possible influence of interactions with the outside loops as well as for electrostatic interactions, we have assumed a generous threshold of 50 kcal/mol in relative conformational energy for selection of the potentially low-energy complexes of AII with AT-1. Our calculations found 11 of them, which converged into four geometrically similar "families" according to the "global" spatial positions of AII.

### *Validation/Selection of the Most Plausible 3D Model of the Complex*

Table 1 summarizes the current data on the AT-1 mutants (mostly for the rat AT-1 receptor) that have been tested for binding of extracellular peptide ligands (mostly AII) (26–33), intracellular ligand binding (binding to a heterotrimeric G-protein (34)) (35–39), and for IP production (10, 31–33, 40–49). Generally, it was shown that the positions most sensitive to extracellular ligand binding are those occupied in the wild-type (WT) receptor by I14, H24, Y26, I27, T88, M90, Y92, K102, H166, R167, V179, H183, Y184, E185, K199, F259, T260, D262, H272, D278, D281, and N295 (shown in bold italics in Table 1). The positions mostly

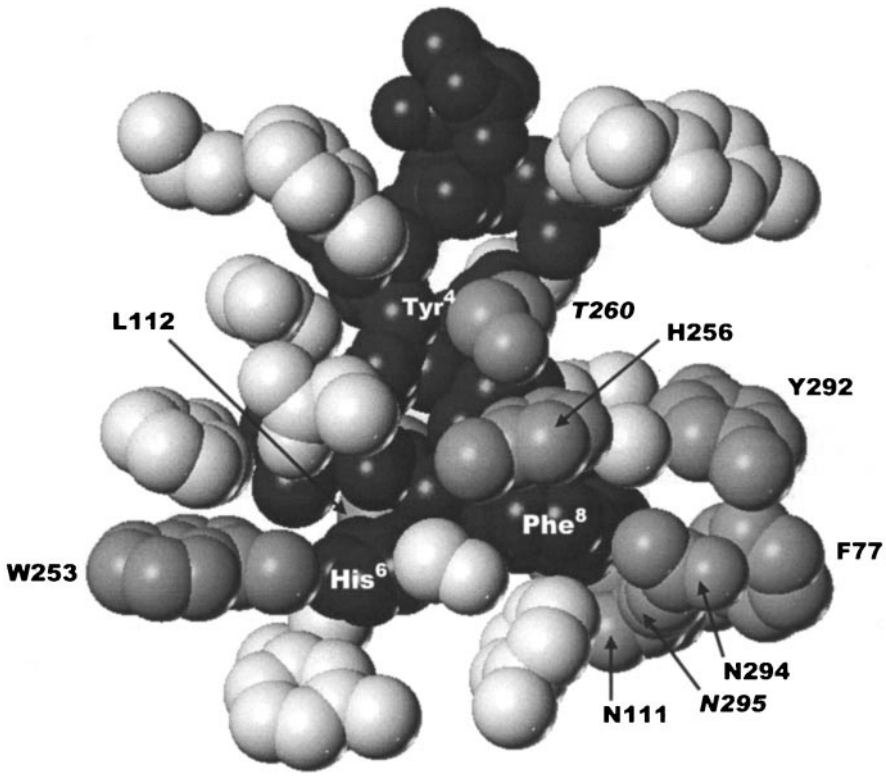


**FIG. 1.** Packing of AII (space-filling models in black) within AT-1. The AT-1 residues in nearest vicinity of AII are shown in dark gray (residues involved in ligand binding or signal transduction; those residues are labeled in black), or in light gray. Only side chains of the AT-1 residues are shown. The functionally important residues of AII are labeled in white. Note L112 residue located behind AII.

sensitive to IP production are those occupied in WT by F77, L78, S107, F110, N111, S115, L118, M142, L143, P162, E173, A181, I193, L195, T198, I245, W253, V254, H256, Y292, N294, and L305 (shown in bold in Table 1). Several residues have been shown as the most important for constitutive activity, namely F77, N111, L112, L118, L195, and I245 (also shown in bold in Table 1). Totally, 23 residues were shown to be involved in signal transduction or in manifestation of constitutive activity, 19 of them being located in the TM region of the AT-1 receptor. 22 residues were shown to be involved in external ligand binding; only seven of them are located in the TM region of the AT-1 receptor.

With some caveats (for instance, different positions in AT-1 may be important for binding of different extracellular ligands (26, 28)), the data of site-directed mutagenesis collected in Table 1 may be used for selection and independent validation of the most plausible 3D model for the AII–AT1 complex. Table 2 lists the interatomic contacts (<4.0 Å) between all residues of AII and AT-1 in all four possible families of the AII–AT-1 complexes obtained by our calculations (the order of families is arbitrary). For each family, the AT-1 residues involved in signal transduction or in constitutive activity according to the data of site-directed mutagenesis are shown in bold, and residues possibly involved in ligand binding are shown in bold italics, respectively. Shaded areas in Table 2 correspond to AII moieties that are most important for displaying agonistic activity of AII analogs, namely to $Tyr^4$, $His^6$, $Phe^8$, and the C-terminal carboxyl. In a quite reasonable assumption that the residues of AII, that are most important for agonist activity, are more likely to contact the AT-1 residues involved into either signal transduction or constitutive activity, the most plausible model for the AII–AT-1 complex is that corresponding to family 2. Interestingly, this particular model also possesses the lowest energy according to our calculations (−476.3 kcal/mol in the selected force field). In terms of conformational energy, AII interacts primarily with TM helices III and VI (energies of interaction are −26.3 and −23.9 kcal/mol, respectively), then with helices V and VII (−15.3 and −14.4 kcal/mol), and then with the helix II (−5.0 kcal/mol); interactions with helices I and IV are practically absent.

Figure 1 shows that the selected model provides a well-packed structure with significant penetration of the crucial $Phe^8$ residue of AII inside the helical bundle. The nearest environment of the functionally important $Tyr^4$, $His^6$, and $Phe^8$ residues includes seven residues of AT-1, which are known to be involved in

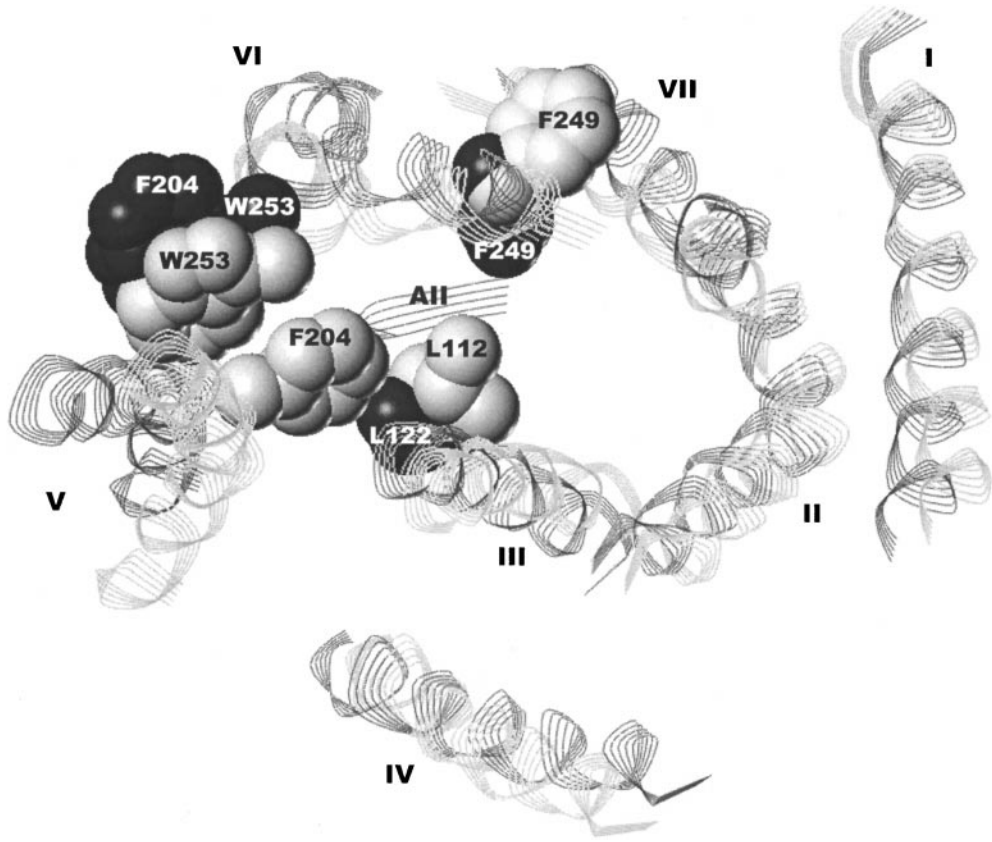


**FIG. 2.** Overlapped 3D structures of the TM region of AT-1 (light gray ribbons) and the AII –AT complex (dark gray ribbons) as viewed from the intracellular side of the membrane. AII and TM helices are labeled in black. Selected side chains in AT-1 (space-filled models in light gray, labeled in black) and in the AII–AT-1 complex (space-filled models in black, labeled in white) are shown. Note the W253 side chain in the AII–AT-1 complex located behind the F204 side chain.

signal transduction or constitutive activity, namely F77, N111, L112, W253, H256, Y292, and H294. The Tyr[4] residue presumably interacts also with the corresponding residues in the extracellular loops.

Figure 2 depicts the view from the intracellular side to the selected 3D model of the AII–AT-1 complex in comparison with the model of the TM helical bundle of AT-1 optimized without AII (two helices noninteracting with AII, I and IV, are overlapped in Fig. 2). Generally, "global" movements of helices as rigid bodies to accommodate the ligand are small, the corresponding overall rmsd value being 1.83 Å. This is in line with the experimentally observed small movements of TM helices in BR upon transitions from the "dark" to the "light" states (50–52). However, as is evident from Fig. 2, the movements of the ends of the individual helices within the bundle may be rather significant, especially for the intracellular end of helix V. This observation is in good agreement with the experimental data suggesting that many AT-1 residues most sensitive to interaction with the intracellular ligand, a G-protein, are located in the intracellular loop between helices V and VI ((38); see also Table 1). Also, according to our model, several residues of AT-1 experience significant conformational transitions in their side chains ($\Delta\chi_1$ values greater than 60°) upon binding of AII to AT-1. Those in direct contact with AII, namely L112, F204, F249, and W253, are depicted in Fig. 2.

### *Comparison with 3D Models Suggested by Other Authors*

As it was mentioned above, the early models of the AII–AT-1 complex have been based on 3D structure of BR. The model proposed by the Scheraga and Maigret modeling groups (42, 53) describes the AII–AT-1 complex, where AII adopts the "receptor-bound" conformation predicted by the same groups earlier (54), and this conformation is docked to AT-1 by electrostatic interactions between the $\alpha$- and/or $\beta$-carboxyls of Asp[1] in AII and the side chain of K199 in AT-1 (53). The difference between the "empty" and "occupied" states of AT-1 in this model has been interpreted as the difference between two conformational states where the hydroxyl of the Y292 side chain forms a hydrogen bond either with the $\beta$-carbonyl of N111, or with the

$\beta$-carboxyl of D74 (42). The model by the Inagami group (9, 29) was similar to the previous one, except it used the "receptor-bound" conformation of AII developed by us previously (7, 8). The Inagami model suggested that the Y292 side chain in the "empty" state maintains hydrogen bonding with the N295 side chain, and, upon AII binding, switches to hydrogen bonding with D74, as in the Scheraga/Maigret model. This switching involves concerted rotations of two TM helices, namely helices II and VII (9). The other model, based both on BR and on the rough structure of Rh determined by electron microscopy (17), also has placed K199 in direct interaction with the $\alpha$-carboxyl of $Phe^8$. The model suggests interactions between D281 and $Arg^2$ in AII (32), between H256 and the side chain of $Phe^8$ (32), and between N111 and $Tyr/Phe^4$ (10). This model also utilizes our model of the "receptor-bound" conformation of AII, as well as the model proposed by the Paiva/Oliveira group (3), which was also based on the rough structure of Rh. In this model, AII interacts with K199 and D281 in the same way as described above; $Tyr^4$ is inserted into the transmembrane pocket, but not interacts with N111 directly. The authors have developed this model further taking into account the G-protein activation (55), and the much more detailed X-ray structure of Rh (see the URL address http://www.gpcr.org/7tm/models/oliveira/index.html). The most recent 3D model of AT-1 is also based on the Rh structure and on the binding data for the Bpa-containing analogs of AII (13). In this model, the fully extended structure of AII is deeply immersed in the TM region, with $Val^3$ interacting with I172, and $Phe^8$ interacting with F293 and N294.

One main difference between our model and all of the previous models (except the last one (13)) is that our model places $Phe^8$, but not $Tyr^4$, in direct vicinity of the extremely important residues N111, H256, Y292, N294, and N295 deeply buried inside the TM helical bundle of AT-1. This seems more consistent with the experimental results showing that the photolabeled analog [$Bpa^8$]-AII binds AT-1 in the 285–295 region (14). The deep immersion into the TM bundle of $Phe^8$, and not $Tyr^4$ also agrees with the very recent experimental observation that among many dimers of AII obtained by bridging various side chains via aliphatic $\omega$-amino carboxylic acid linkers, only those linked through position 4 displayed sub-micromolar affinities when binding to AT-1 receptors (15). Another significant difference is that conformational transition from the "empty" to "occupied" states of AT-1 in our model is not limited to any specific inter-residue interaction, as Y292–D74. Instead, our model views the process of signal transduction through the TM region of AT-1 as a chain of cooperative conformational perturbations of many side chains, which is initiated by those residues directly affected by binding of AII. According to this paradigm, sensitivity of a given receptor residue to ligand binding, or to signal transduction does not mean that this residue should necessarily be in direct contact with the bound ligand; there may be many pathways to involve these residues in conformational transitions. The on-going site-directed mutagenesis studies would certainly identify new residues involved in signal transduction in AT-1; this is one more reason not to be confined by a model considering only one possible pathway for this process. In fact, we have recently suggested several new "signal transduction" residues in the TM region of AT-1 based on conformational studies of the AT-1 mutants showing constitutive activity, namely residues Y35, L119, F249, S252, I288, N295, and N298 (56).

## CONCLUSION

This study is the first one presenting 3D models of the AII–AT-1 complex obtained by steric and energy considerations only, without prior knowledge of the experimental results of site-directed mutagenesis for the AT-1 receptor mutants. Therefore, the available data of site-directed mutagenesis could be used for independent validation of the suggested models, which singled out one of the models as the most plausible. No other model of the AII–AT-1 complex described in the literature allows such validation, since all of them use the data on the AT-1 mutants beforehand. Also, no other approach offers several 3D models of the AII–AT-1 complex for further evaluation. Our final 3D model of the complex of AII and the TM helical bundle of AT-1 brings in contact the residues of AII responsible for agonistic activity, $Tyr^4$, $His^6$, and $Phe^8$, and many residues of AT-1 involved in signal transduction according to the data of site-directed mutagenesis. The model predicts the existence of several possible conformational pathways for transferring signal through the TM region of AT-1.

## ACKNOWLEDGMENTS

The authors acknowledge support for this research from NIH Grants EY12113 and GM53630.

## REFERENCES

1. de Gasparo, M., Catt, K. J., Inagami, T., Wright, J. W., and Unger, T. (2000) International union of pharmacology. XXIII. The angiotensin II receptors [Review]. *Pharmacol. Rev.* **52,** 415–472.
2. Underwood, D. J., Strader, C. D., Rivero, R., Patchett, A. A., Greenlee, W., and Prendergast, K. (1994) Structural model of antagonist and agonist binding to the angiotensin II, $AT_1$ subtype, G protein coupled receptor. *Chem. Biol.* **1,** 211–221.
3. Paiva, A. C. M., Costa-Neto, C. M., and Oliveira, L. (1998) Molecular modeling and mutagenesis studies of angiotensin II/AT1 interaction and signal transduction. *In* Proceedings of INABIS'98 Conference–5th Internet World Congress on Biomed-

ical Sciences at McMaster University, Posted on the Internet, see http://www.mcmaster.ca/inabis98/escher/paiva0625.

4. Regoli, D., Park, W. K., and Rioux, F. (1974) Pharmacology of angiotensin. *Pharm. Rev.* **26,** 69–123.
5. Duncia, J. V., Chiu, A. T., Carini, D. J., Gregory, G. B., Johnson, A. L., Price, W. A., Wells, G. J., Wong, P. C., Calabrese, J. C., and Timmermans, P. B. M. W. M. (1990) The discovery of potent nonpeptide angiotensin II receptor antagonists: A new class of potent antihypertensives. *J. Med. Chem.* **33,** 1312–1329.
6. Garcia, K. C., Ronco, P. M., Veroust, P. J., Brunger, A. T., and Amzel, L. M. (1992) Three-dimensional structure of an angiotensin II-FAB complex at 3Å: Hormone recognition by an anti-idiotypic antibody. *Science* **257,** 502–507.
7. Nikiforovich, G. V., and Marshall, G. R. (1993) Three-dimensional recognition requirements for angiotensin agonists: A novel solution for an old problem. *Biochem. Biophys. Res. Commun.* **195,** 222–228.
8. Nikiforovich, G. V., Kao, J. L.-F., Plucinska, K., Zhang, W. J., and Marshall, G. R. (1994) Conformational analysis of two cyclic analogs of angiotensin: Implications for the biologically active conformation. *Biochemistry* **33,** 3591–3598.
9. Inoue, Y., Nakamura, N., and Inagami, T. (1997) A review of mutagenesis studies of angiotensin II type 1 receptor, the three-dimensional receptor model in search of the agonist and antagonist binding site and the hypothesis of a receptor activation mechanism [Review]. *J. Hypertension* **15,** 703–714.
10. Noda, K., Feng, Y. H., Liu, X. P., Saad, Y., Husain, A., and Karnik, S. S. (1996) The active state of the $AT_1$ angiotensin receptor is generated by angiotensin II induction. *Biochemistry* **35,** 16435–16442.
11. Hunyady, L., Balla, T., and Catt, K. J. (1996) The ligand binding site of the angiotensin $AT_1$ receptor [Review]. *Trends Pharmacol. Sci.* **17,** 135–140.
12. Pertihnhez, T. A., Nakaie, C. R., Paiva, A. C. M., and Schreier, S. (1997) Spin-labeled extracellular loop from a seven-transmembrane helix receptor: Studies in solution and interaction with model membranes. *Biopolymers* **42,** 821–829.
13. Boucard, A. A., Wilkes, B. C., Laporte, S. A., Escher, E., Guillemette, G., and Leduc, R. (2000) Photolabeling identifies position 172 of the human $AT_1$ receptor as a ligand contact point: Receptor-bound angiotensin II adopts an extended structure. *Biochemistry* **39,** 9662–9670.
14. Laporte, S. A., Boucard, A. A., Servant, G., Guillemette, G., Leduc, R., and Escher, E. (1999) Determination of peptide contact points in the human angiotensin II type I receptor ($AT_1$) with photosensitive analogs of angiotensin II. *Mol. Endocrinol.* **13,** 578–586.
15. Therrien, K. A., Deraet, M., Dubois, A., Rihakova, L., Kitas, E. A., Meister, W., Speth, R., and Escher, E. (2001) Tools for the identification of receptor dimers: Synthesis and biological evaluation of on-resin dimerized, photosensitive analogues of angiotensin II. *In* Abstracts of the Seventeenth American Peptide Symposium (Hougthen, R., and Lebl, M., Eds.), p. A134, San Diego.
16. Sander, C., and Schneider, R. (1991) Database of homology derived protein structures and the structural meaning of sequence alignment. *Proteins* **9,** 56–68.
17. Baldwin, J. M. (1993) The probable arrangement of the helices in G protein-coupled receptors. *EMBO J.* **12,** 1693–1703.
18. Palczewski, K., Takashi, K., Tetsuya, H., Behnke, C., Motoshima, H., Fox, B., Le Trong, I., Teller, D., Okada, T., Stenkamp, R., Yamamoto, M., and Miyano, M. (2000) Crystal structure of rhodopsin: A G-protein-coupled receptor. *Science* **289,** 739–745.
19. Nikiforovich, G. V. (1998) A novel nonstatistical method for predicting breaks in transmembrane helices. *Protein Eng.* **11,** 279–283.
20. Nikiforovich, G. V., Hruby, V. J., Prakash, O., and Gehrig, C. A. (1991) Topographical requirements for delta-selective opioid peptides. *Biopolymers* **31,** 941–955.
21. Nikiforovich, G. V., Galaktionov, S., Balodis, J., and Marshall, G. R. (2001) Novel approach to computer modeling of seven-helical transmembrane proteins: Current progress in test case of bacteriorhodopsin. *Acta Biochimica Polonica* **48,** 53–64.
22. Dunfield, L. G., Burgess, A. W., and Scheraga, H. A. (1978) Energy parameters in polypeptides. 8. Empirical potential energy algorithm for the conformational analysis of large molecules. *J. Phys. Chem.* **82,** 2609–2616.
23. Nemethy, G., Pottle, M. S., and Scheraga, H. A. (1983) Energy Parameters in polypeptides. 9. Updating of geometrical parameters, nonbonded interactions, and hydrogen bond interactions for the naturally occurring amino acids. *J. Phys. Chem.* **87,** 1883–1887.
24. Vakser, I. A., and Nikiforovich, G. V. (1995) Protein docking in the absence of detailed molecular structures. *In* Methods in Protein Structure Analysis (Atassi, M. Z., Ed.), pp. 505–514, Plenum Press, New York.
25. Pebay-Peyroula, E., Rummel, G., Rosenbusch, J. P., and Landau, E. M. (1997) X-ray structure of bacteriorhodopsin at 2.5 angstroms from microcrystals grown in lipidic cubic phases. *Science* **277,** 1676–1681.
26. Schambye, H. T., Hjorth, S. A., Bergsma, D. J., Sathe, G., and Schwartz, T. W. (1994) Differentiation between binding sites for angiotensin II and nonpeptide antagonists on the angiotensin II type 1 receptors. *Proc. Natl. Academy of Sci. USA* **91,** 7046–7050.
27. Schambye, H. T., Vonwijk, B., Hjorth, S. A., Wienen, W., Entzeroth, M., Bergsma, D. J., and Schwartz, T. W. (1994) Mutations in transmembrane segment VII of the $AT_1$ receptor differentiate between closely related insurmountable and competitive angiotensin antagonists. *Br. J. Pharmacol.* **113,** 331–333.
28. Hjorth, S. A., Schambye, H. T., Greenlee, W. J., and Schwartz, T. W. (1994) Identification of peptide binding residues in the extracellular domains of the $AT_1$ receptor. *J. Biol. Chem.* **269,** 30953–30959.
29. Yamano, Y., Ohyama, K., Kikyo, M., Sano, T., Nakagomi, Y., Inoue, Y., Nakamura, N., Morishima, I., Guo, D. F., Hamakubo, T., and Inagami, T. (1995) Mutagenesis and the molecular modeling of the rat angiotensin II receptor ($AT_1$). *J. Biol. Chem.* **270,** 14024–14030.
30. Noda, K., Saad, Y., Kinoshita, A., Boyle, T. P., Graham, R. M., Husain, A., and Karnik, S. S. (1995) Tetrazole and carboxylate groups of angiotensin receptor antagonists bind to the same subsite by different mechanisms. *J. Biol. Chem.* **270,** 2284–2289.
31. Noda, K., Saad, Y., and Karnik, S. S. (1995) Interaction of $Phe^8$ of angiotensin II with $Lys^{199}$ and $His^{256}$ of $AT_1$ receptor in agonist activation. *J. Biol. Chem.* **270,** 28511–28514.
32. Feng, Y. H., Noda, K., Saad, Y., Liu, X. P., Husain, A., and Karnik, S. S. (1995) The docking of $Arg^2$ of angiotensin II with $Asp^{281}$ of $AT_1$ receptor is essential for full agonism. *J. Biol. Chem.* **270,** 12846–12850.
33. Monnot, C., Bihoreau, C., Conchon, S., Curnow, K. M., Corvol, P., and Clauser, E. (1996) Polar residues in the transmembrane domains of the type 1 angiotensin II receptor are required for binding and coupling–reconstitution of the binding site by co-expression of two deficient mutants. *J. Biol. Chem.* **271,** 1507–1513.
34. Horn, F., van der Wenden, E. M., Oliveira, L., Ijzerman, A. P., and Vriend, G. (2000) Receptors coupling to G proteins: Is there a signal behind the sequence? *Proteins* **41,** 448–459.

35. Sano, T., Ohyama, K., Yamano, Y., Nakagomi, Y., Nakazawa, S., Kikyo, M., Shirai, H., Blank, J. S., Exton, J. H., and Inagami, T. (1997) A domain for G protein coupling in carboxyl-terminal tail of rat angiotensin II receptor type 1a. *J. Biol. Chem.* **272,** 23631–23636.

36. Miura, S., Zhang, J., and Karnik, S. S. (2000) Angiotensin II type 1 receptor-function affected by mutations in cytoplasmic loop CD. *FEBS Lett.* **470,** 331–335.

37. Tang, H., Guo, D. F., Porter, J. P., Wanaka, Y., and Inagami, T. (1998) Role of cytoplasmic tail of the type 1A angiotensin II receptor in agonist- and phorbol ester-induced desensitization. *Circulation Res.* **82,** 523–531.

38. Conchon, S., Barrault, M.-B., Miewrey, S., Corvol, P., and Clauser, E. (1997) The C-terminal third intracellular loop of the rat $AT_{1A}$ angiotensin receptor plays a key role in G protein coupling specificity and transduction of the mitogenic signal. *J. Biol. Chem.* **272,** 25566–25572.

39. Shibata, T., Suzuki, C., Ohnishi, J., Murakami, K., and Miyazaki, H. (1996) Identification of regions in the human angiotensin II receptor type 1 responsible for $G_i$ and $G_q$ coupling by mutagenesis study. *Biochem. Biophys. Res. Commun.* **218,** 383–389.

40. Miura, S., Feng, Y. H., Husain, A., and Karnik, S. S. (1999) Role of aromaticity of agonist switches of angiotensin II in the activation of the $AT_1$ receptor. *J. Biol. Chem.* **274,** 7103–7110.

41. Bihoreau, C., Monnot, C., Davies, E., Teutsch, B., Bernstein, K. E., Corvol, P., and Clauser, E. (1993) Mutation of $Asp^{74}$ of the rat angiotensin-II receptor confers changes in antagonist affinities and abolishes G-protein coupling. *Proc. Natl. Acad. Sci. USA* **90,** 5133–5137.

42. Marie, J., Maigret, B., Joseph, M. P., Larguier, R., Nouet, S., Lombard, C., and Bonnafous, J. C. (1994) $Tyr^{292}$ in the seventh transmembrane domain of the $AT_{1a}$ angiotensin II receptor is essential for its coupling to phospholipase C. *J. Biol. Chem.* **269,** 20815–20818.

43. Hunyady, L., Ji, H., Jagadeesh, G., Zhang, M., Gaborik, Z., Mihalik, B., and Catt, K. J. (1998) Dependence of $AT_1$ angiotensin receptor function on adjacent asparagine residues in the seventh transmembrane helix. *Molecular Pharmacology* **54,** 427–434.

44. Costa-Neto, C. M., Mikakawa, A. A., Oliveira, L., Hjorth, S. A., Schwartz, T. W., and Paiva, A. C. M. (2000) Mutational analysis of the interaction of the N- and C-terminal ends of angiotensin II with the rat $AT_{1A}$ receptor. *Br. J. Pharmacol.* **130,** 1263–1268.

45. Balmforth, A. J., Lee, A. J., Warburton, P., Donnelly, D., and Ball, S. G. (1997) The conformational change responsible for $AT_1$ receptor activation is dependent upon two juxtaposed asparagine residues on transmembrane helices III and VII. *J. Biol. Chem.* **272,** 4245–4251.

46. Han, H., Shimuta, S. I., Kanashiro, C. A., Oliveira, L., Han, S. W., and Paiva, A. C. M. (1998) Residues $Val^{254}$, $His^{256}$, and $Phe^{259}$ of the angiotensin II $AT_1$ receptor are not involved in ligand binding but participate in signal transduction. *Mol. Endocrinol.* **12,** 810–814.

47. Parnot, C., Bardin, S., Miserey-Lenkei, S., Guedin, D., Corvol, P., and Clauser, E. (2000) Systematic identification of mutations that constitutively activate the angiotensin II type 1a receptor by screening a randomly mutated cDNA library with an original pharmacological bioassays. *Proc. Natl. Acad. Sci. USA* **97,** 7615–7620.

48. Feng, Y.-H., Miura, S., Husain, A., and Karnik, S. S. (1998) Mechanism of constitutive activation of the $AT_1$ receptor: Influence of the size of the agonist switch binding residue $Asn^{111}$. *Biochemistry* **37,** 15791–15798.

49. Groblewski, T., Maigret, B., Larguier, R., Lombard, C., Bonnafous, J.-C., and Marie, J. (1997) Mutation of $Asn^{111}$ in the third transmembrane domain of the $AT_{1A}$ angiotensin ii receptor induces its constitutive activation. *J. Biol. Chem.* **272,** 1822–1826.

50. Luecke, H., Richter, H. T., and Lanyi, J. K. (1998) Proton transfer pathways in bacteriorhodopsin at 2.3 angstrom resolution. *Science* **280,** 1934–1937.

51. Oka, T., Kamikubo, H., Tokunaga, F., Lanyi, J. K., Needleman, R., and Kataoka, M. (1999) Conformational change of helix G in the bacteriorhodopsin photocycle: investigation with heavy atom labeling and X-ray diffraction. *Biophys. J.* **76,** 1018–1023.

52. Sass, H. J., Buldt, G., Gessenich, R., Hehn, D., Neff, D., Schlesinger, R., Berendzen, J., and Ormos, P. (2000) Structural alterations for proton translocation in the M state of wild-type bacteriorhodopsin. *Nature* **406,** 649–653.

53. Joseph, M.-P., Maigret, B., and Scheraga, H. A. (1995) Proposals for the angiotensin II receptor-bound conformation by comparative computer modeling of AII and cyclic analogs. *Int. J. Pept. Prot. Res.* **46,** 514–526.

54. Joseph, M. P., Maigret, B., Bonnafous, J. C., Marie, J., and Scheraga, H. A. (1995) A computer modeling postulated mechanism for angiotensin II receptor activation. *J. Protein Chem.* **14,** 381–398.

55. Oliveira, L., Paiva, A. C. M., and Vriend, G. (1999) A low resolution model for the interaction of G proteins with G protein-coupled receptors [Review]. *Protein Eng.* **12,** 1087–1095.

56. Nikiforovich, G. V., and Marshall, G. R. (2001) Conformational model of signal transduction in the transmembrane region of the AT-1 receptor. *In* Abstracts of the Seventeenth American Peptide Symposium (Hougthen, R., and Lebl, M., Eds.), p. A137, San Diego.